Joint International Topical Meeting on Mathematics & Computation and Supercomputing in Nuclear Applications (M&C + SNA 2007)
Monterey, California, April 15-19, 2007, on CD-ROM, American Nuclear Society, LaGrange Park, IL (2007)

THE DOPPLER-DEFECT BENCHMARK: OVERVIEW AND SUMMARY OF RESULTS

Russell D. Mosteller
Los Alamos National Laboratory
Los Alamos, NM 87545
mosteller@lanl.gov

ABSTRACT

A set of computational benchmarks for the Doppler reactivity defect has been specified for fuel pin cells containing normal or enriched UO_2 fuel, reactor-recycle mixed-oxide (MOX) fuel, or weapons-grade MOX fuel. This Doppler benchmark has been approved by the Joint Benchmark Committee of the Mathematics and Computations, Reactor Physics, and Radiation Protection and Shielding Divisions of the American Nuclear Society. This paper describes the benchmark specifications and provides a succinct summary of the results submitted for it. Some of those results are described in more detail in individual companion papers submitted by the participants. The complete set of benchmark specifications is provided in Appendix A.

Key Words: MOX, UO_2, Doppler, Benchmark, Overview, Summary

1. INTRODUCTION

The Doppler coefficient of reactivity is a crucial parameter in the evaluation of several transients for light water reactors (LWRs), including the control-rod-ejection and steamline-break accidents in pressurized water reactors (PWRs). However, it is relatively small in magnitude: Doppler feedback in going from hot zero power (HZP) to hot full power (HFP) in an LWR produces a reactivity change of only about 1000 pcm. Furthermore, that reactivity change cannot be measured directly in an operating reactor but instead must be inferred from a combination of other parameters.

Taken together, these factors produce a relatively large uncertainty in the Doppler coefficient of reactivity. An uncertainty of approximately 10% in the Doppler coefficient traditionally has been assumed in LWR safety analyses to produce an acceptably conservative model. Recently, that concern has been compounded by the contributions from plutonium isotopes, both in mixed-oxide fuel and in high-burnup UO_2 fuel.

To address that concern, a set of computational benchmarks for the Doppler reactivity defect has been created [1]. The set also serves as benchmarks for the Doppler coefficient of reactivity, since it is simply the reactivity defect divided by the change in fuel temperature. The benchmarks are relatively simple but retain all of the important contributors to Doppler reactivity feedback. They are based on previous benchmark studies [2,3] but extend them to higher enrichments and MOX concentrations and to weapons-grade MOX configurations. The set of benchmarks has been approved by the Joint Benchmark Committee of the Mathematics

and Computations, Reactor Physics, and Radiation Protection and Shielding Divisions of the American Nuclear Society.

2. BENCHMARK SPECIFICATIONS

The benchmark specifications contain corresponding pairs of pin cells for hot zero power (HZP) and hot full power (HFP) conditions. At HZP, the temperature for everything – fuel, cladding, and borated moderator – is a uniform 600 K. At HFP, the fuel temperature is 900 K, while the temperature of everything else still is 600 K. The Doppler defect is calculated as the reactivity difference between HFP and HZP conditions. The Doppler coefficient of reactivity then is determined as

$$DC = \frac{\Delta \rho_{Dop}}{\Delta T_{Fuel}}$$

where DC is the Doppler coefficient of reactivity, ΔT_{Fuel} is 300 K, and the Doppler defect is

$$\Delta \rho_{Dop} = \frac{k_{HFP} - k_{HZP}}{k_{HFP} * k_{HZP}}$$

There are three subsets of benchmarks, but the pin cells for all three are identical except for the fuel they contain. The first subset contains UO_2 fuel, ranging from normal to 5.0 wt.% enriched uranium. The second subset contains reactor-recycle MOX, with 1 wt.% to 8 wt.% PuO_2, with plutonium isotopics taken from a previous specification.[2] The third subset contains weapons-grade MOX with 1 wt.% to 6 wt.% PuO_2. The plutonium isotopics for those cases are taken from a recent paper [4]. The plutonium isotopics for the two types of MOX cases are summarized in Table I.

Table I. Plutonium Isotopics (at.%)

Fuel	^{239}Pu	^{240}Pu	^{241}Pu	^{242}Pu
Reactor-Recycle MOX	45.0	30.0	15.0	10.0
Weapons-Grade MOX	93.6	5.9	0.4	0.1

The geometry for the benchmarks is an infinite array of identical, infinitely long PWR fuel pin cells with no axial variation. Such an array can be modeled as a single rectangular pin cell with reflecting boundary conditions on the top, bottom, and four sides.

The pin cells are based on an "optimized" fuel assembly design that has been used in both initial and reload cycles of several pressurized water reactors [2], but they have been idealized in a number of ways to simplify the calculations. None of the idealizations have any significant impact on Doppler behavior. First, the fuel is assumed to be pure UO_2 or MOX, with no impurities or fission products present. Second, the enriched uranium is assumed to contain only ^{234}U, ^{235}U, and ^{238}U, with the ^{234}U content proportional to the ^{235}U concentration. Similarly, the MOX fuel is assumed to contain only pure PuO_2 and UO_2, with the Pu containing only the four principal isotopes of plutonium and the uranium being normal uranium. Third, the cladding is taken to be pure zirconium, with no minor constituents of Zircaloy present. Finally, the presence of any structural materials (e.g., spacers) has been ignored. A schematic of the benchmark geometry is given in Fig. 1, and a summary of the specifications is provided in Appendix A.

3. PARTICIPANTS

To date, 44 solutions have been submitted by 15 different organizations in eight countries. Fifteen of those solutions were obtained with Monte Carlo codes, and the other 29 were obtained with deterministic codes. A summary of the participants is given in Tables II and III, along with the codes they used and the source of the nuclear data employed by those codes. For the most part, each combination of code and nuclear data library in those tables corresponds to a different solution. However, some participants submitted multiple solutions using the same code and data that differed in other ways (e.g., geometric approximations, number of energy groups). Some of those results are described in more detail in individual companion papers presented at this conference by the participants.

4. RESULTS

The solutions exhibit some variation in magnitude, but the shapes are quite consistent. Figures 2 through 4 show the average Doppler coefficient for all of the solutions, along with the associated standard deviation for that value. An uncertainty of approximately 10% in the Doppler

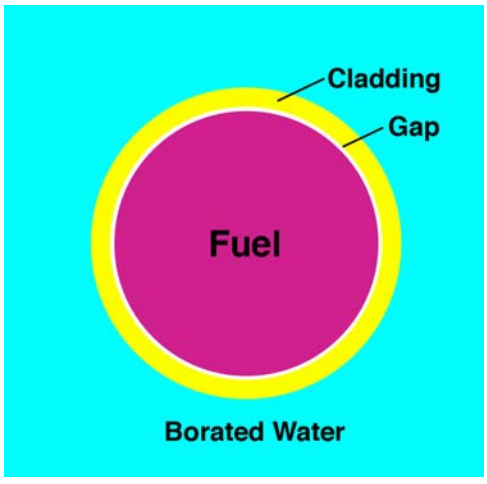

Figure 1. Schematic of the Geometry for the Benchmarks

Table II. Participants Using Monte Carlo Codes for the Doppler Benchmark

Organization	Country	Code	Nuclear Data Libraries
GRS	Germany	MCNP4C	JEF-2.2, JEFF-3.1
GRS	Germany	KENOREST	JEF-2.2
AERB-SRI*	India	MCNP5	ENDF/B-V, ENDF/B-VI
JAEC	Japan	MVP	JENDL-3.3
INL	USA	MCNP5	ENDF/B-VI, ENDF/B-VII
LANL	USA	MCNP5	ENDF/B-V, ENDF/B-VI, ENDF/B-VII, JEFF-3.1
ORNL	USA	KENO-VI	ENDF/B-VI
U of Michigan	USA	MCNP5	ENDF/B-VI
Westinghouse	USA	MCNP5	ENDF/B-VI, ENDF/B-VII

*Joint effort with IGCAR and BARC of India and Kyungpook National University of South Korea

Table III. Participants Using Deterministic Codes for the Doppler Benchmark

Organization	Country	Code	Nuclear Data Libraries
École Polytechnique	Canada	DRAGON	ENDF/B-VI, IAEA, JEFF-3.1
CEA Cadarache	France	APOLLO-2.8	JEFF-3.1
IRSN	France	APOLLO	JEF-2.2
AREVA NP	Germany*	APOLLO2-A	JEF-2.2, JEFF-3.1
AREVA NP	Germany	CASMO	ENDF/B-IV (modified), JEF-2.2 (modified)
AREVA NP	Germany	NEWT	ENDF/B-V
GRS	Germany	DORTOREST	JEF-2.2
GRS	Germany	HELIOS	ENDF/B-VI
BARC	India	LATTEST	IAEA, JEFF-3.1, JENDL-3.2, ENDF/B-VI
TEPSYS	Japan	CASMO-4E	ENDF/B-VI
RRC-KI	Russia	SUHAM-U	ENDF/B-IV, ENDF/B-V, ENDF/B-VI
ORNL	USA	NEWT	ENDF/B-VI
Westinghouse	USA	PARAGON	ENDF/B-VI, ENDF/B-VII

*Joint effort with AREVA NP of France

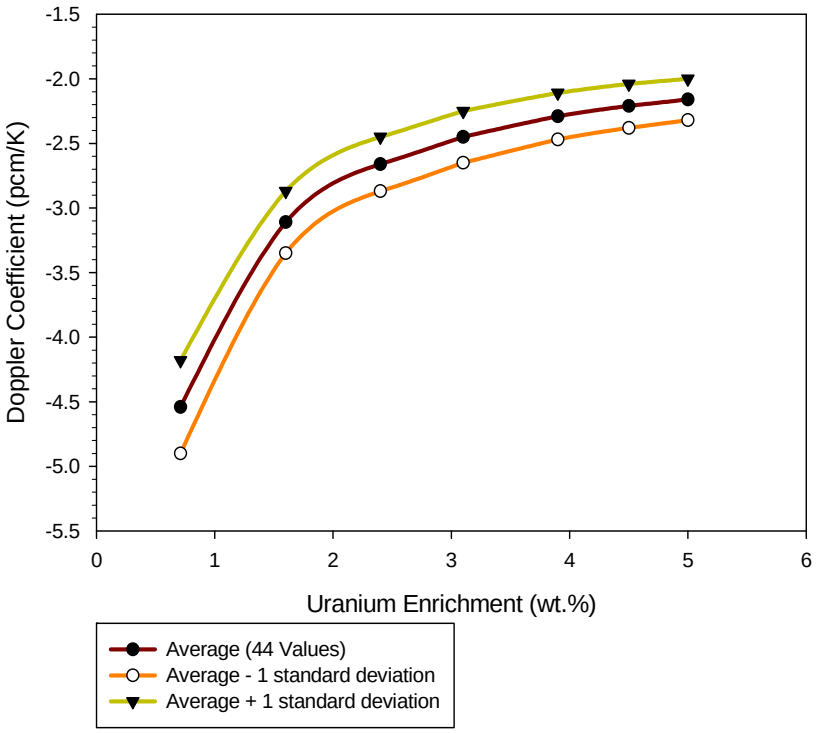

Figure 2. Doppler Coefficient for UO_2 Fuel

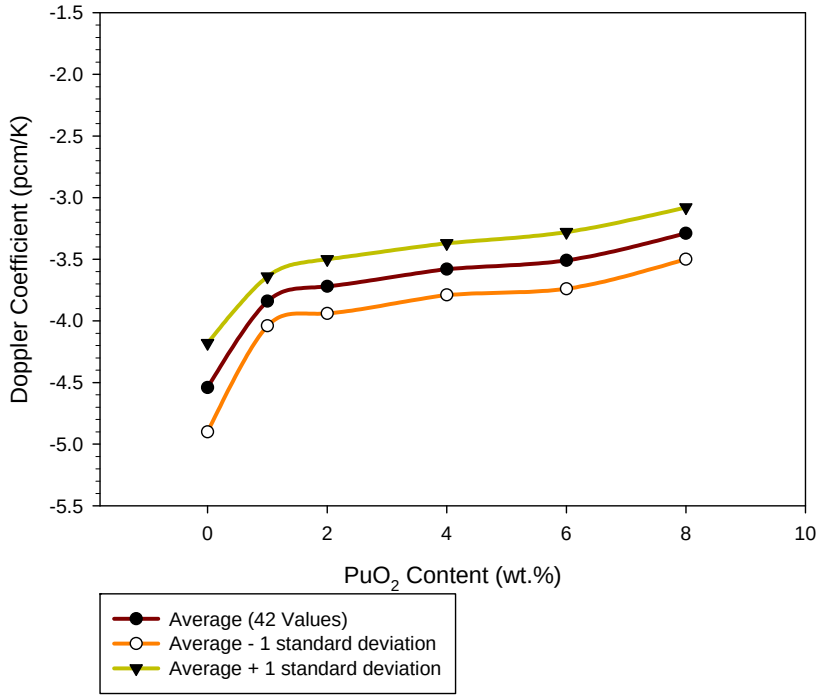

Figure 3. Doppler Coefficient for Reactor-Recycle MOX Fuel.

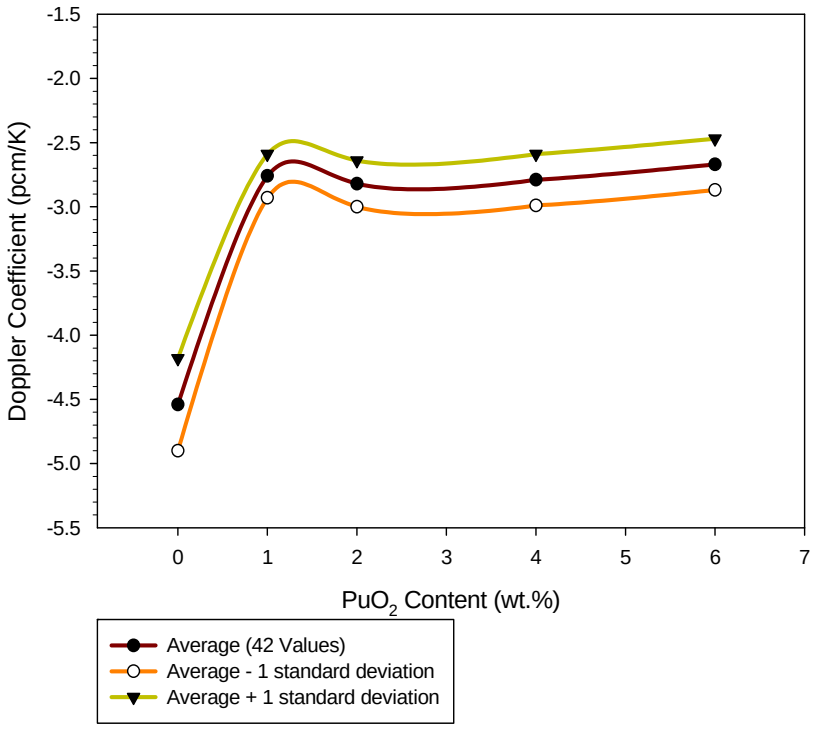

Figure 4. Doppler Coefficient for Weapons-Grade MOX Fuel

coefficient traditionally has been assumed in LWR safety analyses to produce an acceptably conservative model. The standard deviation for every data point in those three figures is less than 10% of the magnitude of the corresponding average value.

The average results for UO_2 and reactor-recycle MOX fuel both produce smooth curves with the Doppler coefficient becoming consistently less negative as the enrichment or PuO_2 content increases, although the change is much smaller for the MOX fuel than for the UO_2 fuel. In contrast, the curve for weapons-grade MOX appears to exhibit oscillatory behavior. That behavior may be illusory, however, because a single straight line could be drawn through the values from 1.0 wt.% MOX to 6 wt.% MOX that stays within a single standard deviation of the average value.

The decrease in the magnitude of the Doppler coefficient for reactor-recycle MOX fuel is much smaller than that for weapons-grade MOX fuel. Furthermore, the Doppler coefficients for both reactor-recycle and weapons-grade MOX fuel show considerably less variation with PuO_2 content than the Doppler coefficient for UO_2 fuel shows with enrichment. Consequently, at least for the fuel loadings in this study, the Doppler coefficients for MOX fuel with high PuO_2 concentrations are significantly more negative than the Doppler coefficients for UO_2 fuel with the higher enrichments.

A number of patterns emerge from a close inspection of the solutions submitted. Two of particular interest are the differences in the results from Monte Carlo and deterministic codes and the differences in the results from different nuclear data libraries.

There are four pairs of results for which an organization submitted results from both a Monte Carlo code and a deterministic code using nuclear data derived from the same nuclear data library. Consequently, differences in the results should be attributable primarily to the methodology employed. Three different Monte Carlo codes and three different deterministic codes were used to generate those solutions. Somewhat surprisingly, the deterministic codes usually produce more negative Doppler coefficients than the Monte Carlo codes. In particular, for three of the four pairs the deterministic code predicts more negative Doppler coefficients than the Monte Carlo code for every case, with differences as large as 24%. For the fourth pair, the deterministic code predicts more negative Doppler coefficients for 11 of the 16 cases, but the maximum difference remains less than 6%. Although no definitive conclusions should be drawn from such a small sample, the pattern and the magnitude of the differences raise some concerns about the consistency of the implemenation of resonance treatments in the two types of codes.

There are five nuclear data libraries for which two or more organizations submitted solutions: ENDF/B-V, ENDF/B-VI, ENDF/B-VII β-2, JEF-2.2, and JEFF-3.1. (ENDF/B-VII β-2 was not available as a general release, but the subsequent general release of ENDF/B-VII.0 did not occur until December 2006). The results for those five nuclear data libraries, averaged over all solutions submitted for them, are shown in Figues 5 through 7. Although clearly there are some differences in magnitude, the shapes of all the curves for a given fuel type are very consistent. ENDF/B-VI consistently produces the most negative Doppler coefficient, and, depending upon the case selected, either ENDF/B-VII β-2 or JEF-2.2 produces the least negative.

5. SUMMARY AND CONCLUSIONS

A set of benchmark specifications has been created for the Doppler reactivity defect. This set has been approved by the Joint Benchmark Committee of the Mathematics and Computations, Reactor Physics, and Radiation Protection and Shielding divisions of the American Nuclear Society. The configurations for the benchmarks are infinite lattices of identical fuel-pin cells at HZP and HFP conditions. The corresponding Doppler coefficient of reactivity can be obtained simply by dividing the Doppler defect from HZP to HFP by the change in the fuel temperature. A complete set of benchmark specifications is provided in Appendix A.

Forty-four separate solutions have been submitted by 15 different organizations in eight different countries. Overall, there is a high level of consistency in the predicted Doppler coefficients, irrespective of the code and nuclear data library employed. Some of those results are described in more detail in individual companion papers presented at this conference by the participants.

REFERENCES

1. R. D. Mosteller, “Computational Benchmarks for the Doppler Reactivity Defect,” LA-UR-06-2968, Los Alamos National Laboratory (April 2006).

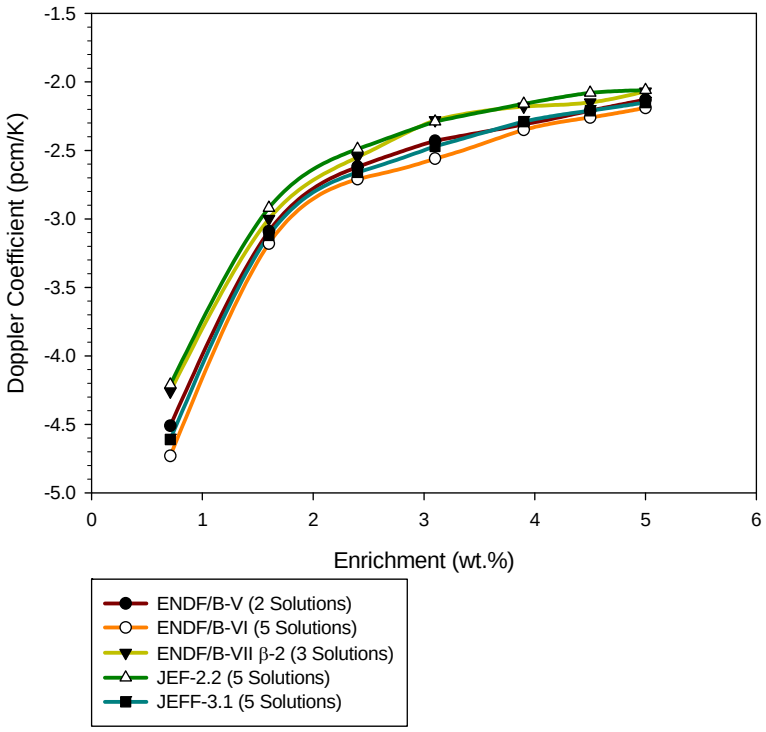

Figure 5. Average Doppler Coefficients for UO_2 Fuel

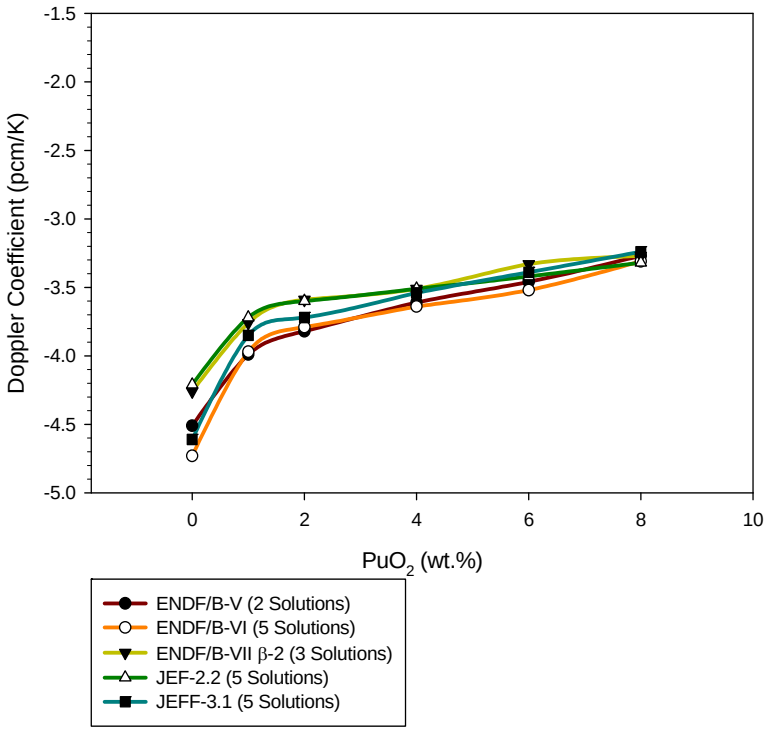

Figure 6. Average Doppler Coefficients for Reactory-Recycle MOX Fuel

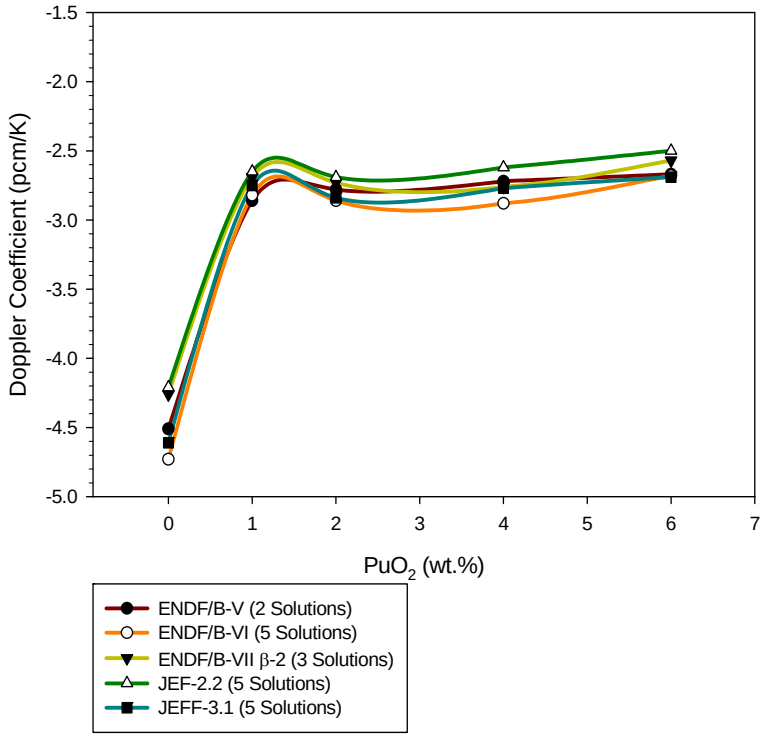

Figure 7. Average Doppler Coefficients for Weapons-Grade MOX Fuel

2. R. D. Mosteller, L. D. Eisenhart, R. C. Little, W. J. Eich, and J. Chao, "Benchmark Calculations for the Doppler Coefficient of Reactivity," *Nucl. Sci. Eng.*, **107**, pp. 265-271 (March 1991).
3. R. D. Mosteller, J. T. Holly, and L. A. Mott, "Benchmark Calculations for the Doppler Coefficient of Reactivity in Mixed-Oxide Fuel," Proceedings of the International Topical *Meeting on Advances in Mathematics, Computations, and Reactor Physics*, CONF-910414, pp. 9.2 1-1–9.2 1-12, Pittsburgh, Pennsylvania (April 1991).
4. G. S. Chang and R. C. Pedersen, "Burnup-Dependent Rim-Effect Comparison of WG-MOX Fuel Pellet in ATR and PWR," *Trans. Am. Nucl. Soc.*, 90, 555 (June 2004).

APPENDIX A. BENCHMARK SPECIFICATIONS

The dimensions and isotopic concentrations for the benchmarks are provided in Tables A-1 through A-8. The only additional information required to set up the benchmark calculations is the number density of the pure zirconium cladding, which is 0.0421838 atoms/b-cm.

Table A-1. Radii and Pitch

Parameter	HZP	HFP
Outer Radius of Fuel (cm)	0.39398	0.39433
Inner Radius of Cladding (cm)	0.40226	0.40226
Outer Radius of Cladding (cm)	0.45972	0.45972
Pitch (cm)	1.26678	1.26678

Table A-2. Atomic Densities for Water at 600 K with 1400 PPM of Boron

Isotope	Number Density (atoms/b-cm)
^{1}H	4.42326×10^{-2}
^{10}B	1.02133×10^{-5}
^{11}B	4.11098×10^{-5}
^{16}O	2.21163×10^{-2}

Table A-3. UO_2 Fuel Composition at 600 K (atoms/b-cm)

Enrichment (wt.%)	^{16}O	^{234}U	^{235}U	^{238}U
0.711	4.61171×10^{-2}	0	1.66029×10^{-4}	2.28925×10^{-2}
1.6	4.61218×10^{-2}	3.00175×10^{-6}	3.73618×10^{-4}	2.26843×10^{-2}
2.4	4.61260×10^{-2}	4.50257×10^{-6}	5.60420×10^{-4}	2.24981×10^{-2}
3.1	4.61297×10^{-2}	5.81576×10^{-6}	7.23867×10^{-4}	2.23352×10^{-2}
3.9	4.61339×10^{-2}	7.31651×10^{-6}	9.10661×10^{-4}	2.21490×10^{-2}
4.5	4.61371×10^{-2}	8.44205×10^{-6}	1.05075×10^{-3}	2.20093×10^{-2}
5.0	4.61397×10^{-2}	9.37998×10^{-6}	1.16749×10^{-3}	2.18930×10^{-2}

Table A-4. UO_2 Fuel Composition at 900 K (atoms/b-cm)

Enrichment (wt.%)	^{16}O	^{234}U	^{235}U	^{238}U
0.711	4.59967×10^{-2}	0	1.65595×10^{-4}	2.28328×10^{-2}
1.6	4.60014×10^{-2}	2.99391×10^{-6}	3.72642×10^{-4}	2.26251×10^{-2}
2.4	4.60056×10^{-2}	4.49081×10^{-6}	5.58956×10^{-4}	2.24393×10^{-2}
3.1	4.60093×10^{-2}	5.80057×10^{-6}	7.21977×10^{-4}	2.22768×10^{-2}
3.9	4.60134×10^{-2}	7.29740×10^{-6}	9.08283×10^{-4}	2.20911×10^{-2}
4.5	4.60166×10^{-2}	8.42000×10^{-6}	1.04801×10^{-3}	2.19519×10^{-2}
5.0	4.60192×10^{-2}	9.35548×10^{-6}	1.16445×10^{-3}	2.18358×10^{-2}

Table A-5. Reactor-Recycle MOX Fuel Composition at 600 K (atoms/b-cm)

MOX Composition (PuO_2 wt.%)	^{16}O	^{235}U	^{238}U
1.0	4.61140×10^{-2}	1.64368×10^{-4}	2.26636×10^{-2}
2.0	4.61108×10^{-2}	1.62708×10^{-4}	2.24347×10^{-2}
4.0	4.61042×10^{-2}	1.59387×10^{-4}	2.19768×10^{-2}
6.0	4.60977×10^{-2}	1.56067×10^{-4}	2.15190×10^{-2}
8.0	4.60912×10^{-2}	1.52746×10^{-4}	2.10611×10^{-2}

MOX Composition (PuO_2 wt.%)	^{239}Pu	^{240}Pu	^{241}Pu	^{242}Pu
1.0	1.03031×10^{-4}	6.86872×10^{-5}	3.43436×10^{-5}	2.28957×10^{-5}
2.0	2.06062×10^{-4}	1.37374×10^{-4}	6.86872×10^{-5}	4.57915×10^{-5}
4.0	4.12123×10^{-4}	2.74749×10^{-4}	1.37374×10^{-4}	9.15830×10^{-5}
6.0	6.18185×10^{-4}	4.12123×10^{-4}	2.06062×10^{-4}	1.37374×10^{-4}
8.0	8.24247×10^{-4}	5.49498×10^{-4}	2.74749×10^{-4}	1.83166×10^{-4}

Table A-6. Reactor-Recycle MOX Fuel Composition at 900 K (atoms/b-cm)

MOX Composition (PuO_2 wt.%)	^{16}O	^{235}U	^{238}U
1.0	4.59936×10^{-2}	1.63939×10^{-4}	2.26044×10^{-2}
2.0	4.59904×10^{-2}	1.62283×10^{-4}	2.23761×10^{-2}
4.0	4.59838×10^{-2}	1.58971×10^{-4}	2.19194×10^{-2}
6.0	4.59773×10^{-2}	1.55659×10^{-4}	2.14628×10^{-2}
8.0	4.59708×10^{-2}	1.52347×10^{-4}	2.10061×10^{-2}

MOX Composition (PuO_2 wt.%)	^{239}Pu	^{240}Pu	^{241}Pu	^{242}Pu
1.0	1.02762×10^{-4}	6.85079×10^{-5}	3.42539×10^{-5}	2.28360×10^{-5}
2.0	2.05524×10^{-4}	1.37016×10^{-4}	6.85079×10^{-5}	4.56719×10^{-5}
4.0	4.11047×10^{-4}	2.74031×10^{-4}	1.37016×10^{-4}	9.13438×10^{-5}
6.0	6.16571×10^{-4}	4.11047×10^{-4}	2.05524×10^{-4}	1.37016×10^{-4}
8.0	8.22094×10^{-4}	5.48063×10^{-4}	2.74031×10^{-4}	1.82688×10^{-4}

Table A-7. Weapons-Grade MOX Fuel Composition at 600 K (atoms/b-cm)

MOX Composition (PuO_2 wt.%)	^{16}O	^{235}U	^{238}U
1.0	4.61154×10^{-2}	1.64368×10^{-4}	2.26636×10^{-2}
2.0	4.61136×10^{-2}	1.62708×10^{-4}	2.24347×10^{-2}
4.0	4.61099×10^{-2}	1.59387×10^{-4}	2.19768×10^{-2}
6.0	4.61061×10^{-2}	1.56067×10^{-4}	2.15190×10^{-2}

MOX Composition (PuO_2 wt.%)	^{239}Pu	^{240}Pu	^{241}Pu	^{242}Pu
1.0	2.14958×10^{-4}	1.35497×10^{-5}	9.18623×10^{-7}	2.29656×10^{-7}
2.0	4.29916×10^{-4}	2.70994×10^{-5}	1.83725×10^{-6}	4.59312×10^{-7}
4.0	8.59831×10^{-4}	5.41988×10^{-5}	3.67449×10^{-6}	9.18623×10^{-7}
6.0	1.28975×10^{-3}	8.12982×10^{-5}	5.51174×10^{-6}	1.37794×10^{-6}

Table A-8. Weapons-Grade MOX Fuel Composition at 900 K (atoms/b-cm)

MOX Composition (PuO_2 wt.%)	^{16}O	^{235}U	^{238}U
1.0	4.59950×10^{-2}	1.63939×10^{-4}	2.26044×10^{-2}
2.0	4.59932×10^{-2}	1.62283×10^{-4}	2.23761×10^{-2}
4.0	4.59895×10^{-2}	1.58971×10^{-4}	2.19194×10^{-2}
6.0	4.59857×10^{-2}	1.55659×10^{-4}	2.14628×10^{-2}

MOX Composition (PuO_2 wt.%)	^{239}Pu	^{240}Pu	^{241}Pu	^{242}Pu
1.0	2.14397×10^{-4}	1.35143×10^{-5}	9.16224×10^{-7}	2.29056×10^{-7}
2.0	4.28793×10^{-4}	2.70286×10^{-5}	1.83245×10^{-6}	4.58112×10^{-7}
4.0	8.57586×10^{-4}	5.40572×10^{-5}	3.66490×10^{-6}	9.16224×10^{-7}
6.0	1.28638×10^{-3}	8.10859×10^{-5}	5.49735×10^{-6}	1.37434×10^{-6}